Simulation of ultrafast heating induced structural dynamics using a one-dimensional spring model

Junjie Li, Rick Clinite, Xuan Wang, and Jianming Cao*
Department of Physics and National High Magnetic Field Laboratory, Florida State University, Tallahassee, Florida 32310, USA
(Received 21 April 2009; revised manuscript received 3 June 2009; published 22 July 2009)

We developed a one-dimensional spring model to study the dynamics of lattice motion upon ultrafast laser heating. Using this model, we simulated atomic positions as a function of time in a free-standing thin monoatomic metal film as well as in a thin film on a substrate. In particular, we studied how the electronic thermal stress influences lattice expansion after the ultrafast laser heating. The simulation results agree very well with experimental data obtained with femtosecond electron diffraction.

DOI: 10.1103/PhysRevB.80.014304 PACS number(s): 62.30.+d, 61.05.J−, 78.47.jc

I. INTRODUCTION

Structural dynamics initiated by ultrafast laser heating involves the interactions among participating subsystems of charge, spin, and lattice, and has been a subject of intense research for many years. Earlier experimental works utilized femtosecond (fs) optical probes to measure associated modulation in optical properties (transmissivity and/or reflectivity) and extracted the information of structural dynamics through sophisticated theoretical modeling.[1–12] Recent advances in time-resolved x-ray and electron diffraction provide a way to directly monitor these structural dynamics with atomic-level details in real time.[13–20] One main theme of such research concerns primarily laser induced melting under high-pump intensity[10–12,18–20] to gain a microscopic understanding of phase transitions. The others are more focused on reversible structural dynamics, to seek structure-function correlation and the underlying mechanisms driving these dynamics. A widely used model for these reversible structural changes is based on classical continuous elastic equation,[1,15,16,21] which can only provide a limited view of dynamics on the atomic-length scale. So far, simulations of structural dynamics with atomic-level details and comparison of such simulations with time-resolved diffraction data are sparse.

Here, we report a simulation of ultrafast heating induced structural dynamics using a one-dimensional (1D) spring model.[22] It is developed from the classic continuous elastic equation by considering a nanometer film as a chain of point masses connected by springs.[23,24] The simulation provides an atomic-level view of structural dynamics by revealing the position of each point mass (atom) as a function of time for a given temperature (stress) profile. In particular, we studied the role of electronic thermal stress on lattice motion by comparing the simulation results with and without its presence. The simulation fits the data of our femtosecond electron diffraction very well and shows again that electronic thermal stress is essential for driving coherent lattice vibrations.

II. THEORY AND COMPUTATIONAL METHODS

An ultrafast heating process usually involves redistribution of energy deposited by fs optical pulses among different subsystems and can be characterized by several characteristic time scales. For metals without magnetic ordering, the energy of a pump pulse is first absorbed by the electron subsystem via hot electron generation. These hot electrons then thermalize with conduction electrons via strong electron-electron scattering and establish an elevated electron temperature (T_e) in a sub-ps time scale. T_e is usually much higher than the lattice temperature (T_l). Subsequently, electrons transfer their energy to the lattice via electron-phonon (*e-ph*) coupling and finally the two subsystems reach a new thermal equilibrium in a few ps. In general, this ultrafast thermalization process builds up thermal stress from both electronic and lattice heating faster than that the lattice can respond (acoustic phonon period) and therefore can launch a coherent lattice motion (coherent acoustic phonons).

In a typical femtosecond electron diffraction (FED) experiment, the sample is a free-standing thin film of a few tens of nanometers thick. The pump optical and probe electron pulses are put nearly collinear and normal to the film surface to maintain fs time resolution. To maintain a uniform excitation of the entire probed region in the lateral direction, the beam diameter of the pump optical pulse is usually set at millimeter scale and is significantly larger than the size of probe electron beam (about 300 μm in diameter).[13] In addition, the time scale for the lateral heat diffusion out of the probed region along the film surface takes 10 ns or longer in metals. Under these conditions, the temperature and its resulting thermal stress depend only on the distance from the film surface. Accordingly, three-dimensional structural dynamics can be reduced to one dimension with the relevant lattice motion along the film normal direction,[1,18] which is described by a 1D elastic equation as:[21,25,26]

$$\frac{\partial^2 u(x,t)}{\partial t^2} = v^2 \frac{\partial^2 u(x,t)}{\partial x^2} - 2\beta \frac{\partial u(x,t)}{\partial t} - \frac{1}{\rho}\frac{\partial \sigma(x,t)}{\partial x} \quad 0 \le x \le L, \tag{1}$$

where $u(x,t)$ is the displacement, ρ is the material density, β is a damping time constant, v is the longitudinal sound speed, and $\sigma(x,t)$ is stress that is determined by the electron temperature $T_e(x,t)$ and the lattice temperature $T_l(x,t)$. For a free-standing thin film, the initial and boundary conditions are:

$$u(x,t)|_{t=0^+} = 0, u_t(x,t)|_{t=0^+} = 0$$

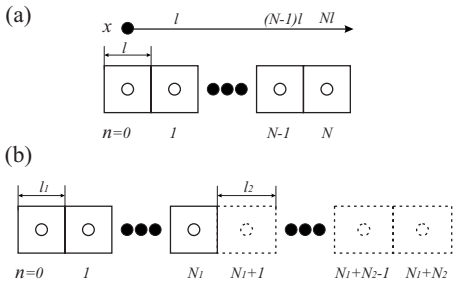

FIG. 1. (a) 1D chain of $N+1$ point masses (atoms). (b) 1D chain of a thin film with N_1+1 point masses on a substrate with N_2 point masses.

$$u_x(x,t)|_{x=0^+} = 0, u_x(x,t)|_{x=L^-} = 0. \tag{2}$$

Once the stress $\sigma(x,t)$ is given, the corresponding structural dynamics in a film relevant to FED experiments [elastic wave $u(x,t)$] can be obtained by solving Eq. (1) under the proper initial and boundary conditions given by Eq. (2). Similarly, the two-dimensional and/or 3D equations can be constructed but we will restrict our discussions to the 1D case that is most relevant to our FED measurements in this paper.

To visualize the motion of each atom and their mutual interactions, the above equations for a 1D continuous film can be converted to the equations for a linear chain of $N+1$ discrete point masses (m) connected by elastic springs, as shown in Fig. 1(a). Define,

$$z_n(t) = u(nl,t),$$

$$p_n(t) = m\frac{d}{dt}z_n(t),$$

$$L = Nl,$$

$$\omega^2 = \frac{C}{\rho l^2} = \frac{v^2}{l^2},$$

$$m = \rho\delta V = \rho l^3,$$

$$\Delta I_n(t) = \left.\frac{m\delta\sigma(x,t)}{\rho\delta x}\right|_{x=nl} = \left.\frac{l^2\delta\sigma(x,t)}{\delta x}l\right|_{x=nl} = l^2\sigma(x,t)\Big|_{\left(n-\frac{1}{2}\right)l}^{\left(n+\frac{1}{2}\right)l}$$

$$I_0(t) = l^2\sigma\left(-\frac{l}{2},t\right)$$

$$I_N(t) = -l^2\sigma\left[\left(N+\frac{1}{2}\right)l,t\right]. \tag{3}$$

where C is the elastic constant along the surface normal direction, l is the effective lattice separation (distance between adjacent point masses), and depends on the lattice orientation. For example, in an Al film of FCC lattice with the surface normal along the [200] direction, a point mass is one Al atom and the effective lattice separation l is just half of a lattice constant 4.05 Å. For more complex structures containing more than one atom per primitive cell, a point mass can be regarded as the center of mass of a primitive cell, and the l is the separation of point masses along a given lattice direction. By substituting Eq. (3) into Eqs. (1) and (2), we reach the equations for a 1D atomic chain

$$\frac{d}{dt}z_n = \frac{p_n}{m},$$

$$\frac{d}{dt}p_0 = \Delta I_0 + I_0 - 2\beta p_0 - m\omega^2(z_0 - z_1),$$

$$\frac{d}{dt}p_N = \Delta I_N + I_N - 2\beta p_N - m\omega^2(z_{N-1} - z_N),$$

$$\frac{d}{dt}p_n = \Delta I_n - 2\beta p_n - m\omega^2(2z_n - z_{n-1} - z_{n+1})(n = 1 \ldots ..N-1),$$

$$z_n(0) = 0, \quad p_n(0) = 0 \quad (n = 1 \ldots ..N-1). \tag{4}$$

In the Eq. (4), the lattice anharmonic contribution is incorporated in the lattice thermal stress. However, the associated displacement is ignored since it is about 2 orders of magnitude smaller than the harmonic term when the sample temperature change is on the order of 100 K. In the following, we will restrict our discussion to this type of ultrafast heating with relatively low lattice temperature rise that is most relevant to the main topic of coherent phonon generation driven by both electronic and lattice heating. However, we would like to emphasize that under the strong excitation conditions, such as laser-induced ultrafast melting with a possible 1000 K lattice temperature jump, the anharmonic contribution can play a crucial role and more sophisticated models should be developed to describe the structural dynamics.[19]

For ultrafast heating of metals, the thermal stress $\sigma(x,t)$ contains the contributions from both lattice and electronic heating:[2,26]

$$\sigma(x,t) = \left\{\begin{array}{ll} \sum_{i=e,l}\gamma_i C_i[T_i(x,t) - T_0] & 0 \le x \le L \\ 0 & x < 0, x > L \end{array}\right\}, \tag{5}$$

where $i=e(l)$ represents electron (lattice), γ_i, C_i, and $T_i(x,t)$ are the corresponding Grüneisen parameter, heat capacity, and the temperature distribution. T_0 is the initial sample base temperature before the optical excitation. As shown in Eq. (5), $\sigma(x,t)$ is determined by the temporal behavior of the electron temperature $[T_e(x,t)]$ and the lattice temperature $[T_l(x,t)]$, which are in turn governed by electron-phonon interactions. In some metals, the kinetics of this energy exchange can be adequately dealt with by invoking the two temperature model (TTM) and choosing the appropriate *e-ph* coupling constant.[27–29] In the following calculation, both $T_e(x,t)$ and $T_l(x,t)$ in Au were calculated by TTM. However, in Al, TTM tends to overestimate the electron-phonon thermalization rate. To eliminate any ambiguity that might be introduced by the theoretical modeling, we used the lattice temperature obtained in FED measurement as $T_l(x,t)$. $T_e(x,t)$ was derived from $T_l(x,t)$ by assuming energy conservation

TABLE I. List of parameters used in the simulation.

Parameters	Al	Au	SiO_2
longitudinal sound velocity $v(m/s)$	6420	3250	5700
Point mass separation $l(\dot{A})$	2.025	2.04	2.70
Electronic Grüneisen constant γ_e	1.6[a]	1.6[b]	
Lattice Grüneisen constant γ_l	2.16[a]	2.96[b]	

[a]Reference 43.
[b]Reference 44.

within the electron and lattice subsystems, $C_e\delta T_e + C_l\delta T_l = \gamma T_e \delta T_e + C_l \delta T_l = E_{\text{pump}} \approx C_l \Delta T$,[13,30] with ΔT as the overall sample temperature jump induced by optical excitation. In a typical FED experiment, ΔT is on the order of 30 K and the Al sample base temperature is about 400 K (room temperature plus laser-induced residual heating). Since ΔT is small and the sample base temperature is very close to the Debye temperature of Al: 428 K (Au: 162 K),[31] the lattice specific heat C_l was taken as a constant in the calculation. In the simulation, the Runge-Kutta method is used to solve the Eqs. (4) and (5) with a step size of 0.02 fs.

III. RESULTS AND DISCUSSIONS

Based on this model, we first simulated the atomic motions in a free-standing 20-nm Al film heated by 50-fs laser pulses. In this case, heating can be safely assumed to be homogeneous across the film after electron thermalization (about 200 fs in Al), considering that in metals the optical penetration depth (e.g., 7.4 nm in Al and 12.9 nm in Au)[32] is comparable to film thickness of 20 nm and the fast energy redistribution across the film can be fulfilled by the ballistic electron transport at a Fermi velocity of $\sim 10^6$ m/s in about 100 fs. This ultrafast electron heating leads to the homogeneous lattice heating via electron-phonon scattering, with T_l reaching its maximum value in Al in about 2 ps once both systems are thermalized. To highlight the general features of atoms' motion and their interaction, the damping parameter β was initially set to 0. When comparing with experimental data, β was floated in the calculation to fit the observed decay of lattice vibration. Other relevant parameters used in the simulation are listed in Table I.

The temporal evolution of the displacement of each atom is shown in Fig. 2 and the average lattice expansion across the film thickness is shown by the solid curve in Fig. 4. Due to homogeneous ultrafast heating across the film, there is no driving force on the inner atoms in the sample film at the beginning due to the lack of thermal gradient. Consequently, the thermal expansion of Al film is initiated from the two open ends and propagates inward in the form of acoustic waves as shown in Fig. 2. These two inward traveling acoustic waves collide and create a standing wave satisfying the open boundary conditions, as shown by the solid curve in Fig. 4. For the standing wave, the period of the fundamental mode is determined by film thickness (L) and longitudinal sound velocity (v), $T=1/f_0=2L/v$. Higher harmonics at frequencies of $(2n+1)f_0$ can also be excited and their relative

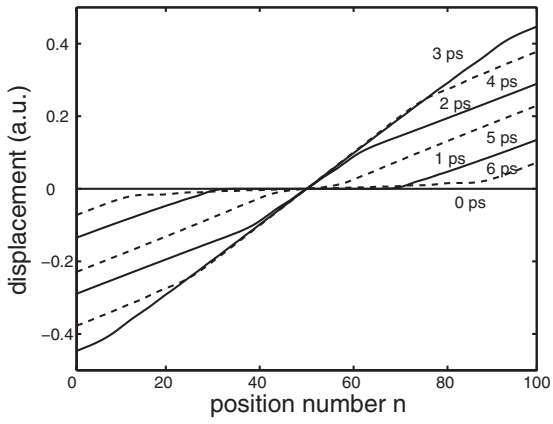

FIG. 2. Atomic displacements to their original equilibrium position in an Al film with $N=100$ at 0, 1, 2, 3, 4, 5, and 6 ps after the optical excitation. The curves at 4, 5, and 6 ps are drawn in dashed lines, indicating that the lattice has passed the point of maximum expansion and started moving back to the new equilibrium position.

weights to the fundamental mode are primarily determined by how fast the thermal stresses σ_e and σ_l are generated. These, in turn, are determined by the electron-electron (about a couple of hundred femtosecond in Al) and *e-ph* (~2 ps in Al) thermalization times, electronic and lattice Grüneisen constants, and the film thickness. Moreover, due to the homogeneity of the thermal stress, the lattice motion is symmetric with respect to the film center. In general, the temporal evolution of the averaged lattice spacing change across the film obtained in the simulation reproduces the general features of structural dynamics observed in our FED measurements.[13]

The model can also be readily modified to simulate the structural dynamics of multilayer samples, such as a thin film on a substrate shown in Fig. 1(b). In this case, the calculation can be done by adding an extra set of parameters representing the substrate and an additional link condition at the interface. The heat diffusion across the interface can also be considered when significant energy transfer across the interface is involved. We take as an example, 10-nm-thick Au on 1-μm-thick SiO_2 substrate, a typical configuration that has been used in many optical pump probe experiments.[7,29,33] Here, pump energy from optical pulse at 800 nm (1.5 eV photon energy) is absorbed only by the Au film. This selective ultrafast heating of Au will launch a coherent acoustic wave and eventually creates a standing wave in Au film satisfying appropriate boundary conditions. In contrast to a free-standing film, the presence of a substrate provides an extra path for heat diffusion from the Au film to the SiO_2 substrate that is driven by their temperature difference. Assuming a good thermal contact at the interface, the associated loss was estimated to be less than 10% of total thermal energy in Au film within the first 60 ps after optical excitation.[34,35] This thermal energy loss will lower the temperature of Au film on the same 10% scale and change the equilibrium lattice position as a function of time. However, the effect of this relatively small temperature drop on coherent phonon damping can be neglected since the decay rate of coherent phonons is a linear function of sample temperature.[36]

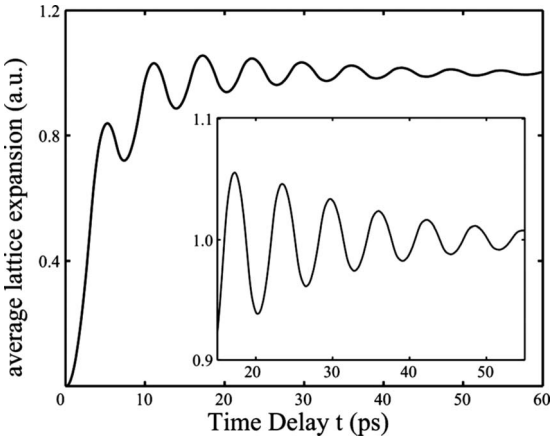

FIG. 3. The average lattice spacing change of 10-nm Au film on a SiO_2 substrate as a function of delay time. The damping induced by the phonon leaking from Au film to SiO_2 substrate is shown in the inset.

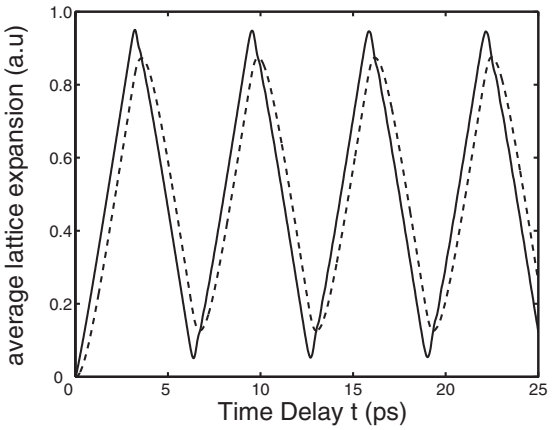

FIG. 4. Comparison of the average lattice spacing change in 20-nm free-standing Al film with (solid line) and without (dashed line) the contribution of electronic thermal stress.

In addition, the presence of SiO_2 substrate introduces another factor contributing to the damping of coherent vibration in Au film due to phonon scattering and transporting at and across the interface. Phonon scattering at interfaces has been a subject of extensive studies dealing with the thermal boundary resistance for many years[37,38] and starts to attract more attentions in recent years since it is a key factor to determine the heat transport in nanoscale devices.[37] These studies reveal that the phonon transport across the interface depends on the acoustic impedances of the two media, which are in turn determined by their mass density and sound velocity, and can be treated by the acoustic mismatch model.[37,38] These parameters are represented by the lattice constant, point mass, and the elastic constant in this 1D model. In our simulation, the acoustic mismatch can be treated by adjusting the arrangements of mass points and the elastic constants in the region to match the actual boundary condition. Here, we used a fairly simple boundary condition to illustrate the effect of damping on the coherent lattice vibrations in Au film due to acoustic wave leaking into the SiO_2 substrate. It is assumed that Au atoms and SiO_2 mass points are arranged collinearly and connected with a spring whose elastic constant is the average of those of Au and SiO_2. In addition, we treat the effective point mass in SiO_2, as a point with the mass of a primitive cell. This simplification excludes the optical phonons but it is justified to describe the acoustic waves with long wavelength (at the center of Brillouin zone) that are excited under the ultrafast heating conditions. In addition, to illustrate this effect on the lattice vibration, we exclude the intrinsic damping parameter β that is related to coherent phonon scattering with thermal phonon bath, conduction electrons, grain boundaries, and defects in a polycrystal metal film.

The simulation results are shown in Fig. 3. In the simulation, the orientation of Au lattice is set along [200] and the corresponding effective lattice spacing and elastic (angular vibrational frequency) constant for Au and SiO_2 are listed in Table I. The *e-ph* coupling was calculated using TTM model and for an overall lattice temperature jump of 100 K, the time constant for the *e-ph* thermalization is 4.2 ps. As displayed in Fig. 3, the temporal evolution of average lattice spacing change displays two distinct features. One is the gradual increase in equilibrium lattice spacing, indicating lattice heating due to electron-phonon coupling. The other is the oscillation around this time-dependent equilibrium position, representing a coherent and in-phase breathing motion of the Au film along the surface normal direction. A unique characteristic associated with this film-on-substrate configuration is the diffusion of acoustic wave from the film into the much thicker substrate. This introduces an extra damping term ($\tau \sim 18$ ps) to the vibration amplitude in the film, as shown in the inset of Fig. 3, despite the thermal energy retained mostly within the Au film. Compared with the 16 ps for the intrinsic damping time constant of coherent vibration observed in a free-standing Al thin film,[13] this leaking induced damping is at the same magnitude if not stronger. Therefore, through careful experimental arrangement and calibration, such as Au film of equal thickness with and without substrate, we should be able to measure and distinguish these two dampings using femtosecond electron diffraction. This will provide a unique approach to measure the mode specific phonon scattering and transporting at and across interfaces, which is a largely unexplored field so far.

Based on this 1D model, we also studied the role of electronic thermal stress on the generation of coherent lattice vibration. Ordinarily, the electronic thermal stress is very small compared with lattice thermal stress and is negligible in normal heating conditions with $T_e = T_l$. However, under ultrafast and nonthermal heating with $T_e \gg T_l$ created by fs optical pulses, the electronic contribution to thermal expansion can be greatly enhanced.[13,39,40] We compared the simulation results of the lattice spacing change with (solid curve) and without (dashed curve) electronic thermal stress. As shown in Fig. 4, they both display some common features such as a nearly identical final equilibrium lattice position. In addition, due to the finite time required for stress build up, the first quarter periods in both simulation sets are elongated and larger than the value of 1.58 ps given by the standing-wave condition. However, there are two obvious distinctions between them. First, the two oscillations are not synchronized in phase, the curve with electronic heating leads about

18° ahead. Second, the lattice vibration amplitude driven by both electron and lattice thermal stresses is about 15% bigger.

These distinctions are signatures of the important role that electronic thermal stress has played in driving coherent lattice vibration. Following optical excitation, the electrons are heated up to a temperature of several thousand degrees, nearly 2 orders of magnitude higher than the lattice temperature, within a couple of hundred femtoseconds in Al. This leads to a domination of electronic thermal stress before *e-ph* thermalization completes a couple of ps later.[13] This transient electronic thermal stress drives the lattice to expand faster initially than when only lattice thermal stress is involved, consequently producing a phase lead in coherent lattice motion. Due to its faster build-up time scale, electronic stress can also excite other higher harmonic acoustic modes and creates a more triangular wave form of lattice vibration, as shown in the solid line in Fig. 4. In addition, the time integral of the electronic thermal stress gives an extra impulse to the lattice to enhance the lattice momentum at early delay time before *e-ph* thermalization, which results in a bigger amplitude of lattice vibration.

We have applied this 1D model to fit the lattice vibration data of FED measurements on a 20-nm free-standing Al film.[13] In this fitting, time zero and temporal evolution of electronic and lattice thermal stress were determined from the lattice temperature curve obtained in FED measurement.[13] To compare with the experimental data, we converted the calculated coherent lattice motion in real space into its correspondent in reciprocal lattice space. Using the atomic positions at a certain time delay obtained by solving Eqs. (4) and (5), the kinematic diffraction intensity as a function of reciprocal vector was calculated by[41]

$$I_s(s,t) = \left| f(s)\sum_{n=0}^{N} \exp\{-s^2 B\{T_l[nl + z_n(t)],\ t)\}/2 + i2\pi s[nl + z_n(t)]\}\right|^2, \quad (6)$$

where $f(s)$ is the atomic scattering factor and normalized to be 1 in our calculations, and $B[T_l,t]$ is the Debye-Waller parameter. In the calculation, the s value that maximizes $I_s(s,t)$ is defined as the new peak center. Take the [200] diffraction peak as an example. After all the atomic positions at a certain time delay were plugged into the Eq. (6), we varied the reciprocal vector s around the original [200] peak position to maximize the intensity $I_s(s,t)$, and the corresponding s was chosen as the new peak center at that time delay. By repeating this at each delay time, the temporal evolution of a given peak center change was obtained.

Then we adjusted the parameters, including the electronic Grüneisen constant γ_e, film thickness N, the lattice temperature change (deposited energy) ΔT, and the damping factor β, to fit the experiment data. The best fitting was obtained with $\gamma_e=1.6$, $N=100$, $\Delta T=29.5°$, and $1/\beta=15$ ps. The uncertainty of γ_e is about ± 0.4. The results are shown as the solid curve in Fig. 5 and agree very well with the experimental data. We also fitted the FED data by excluding electronic thermal stress and setting $\gamma_e=0$, which is shown as the dashed line in Fig. 5. Irrelevant of the values of N, ΔT, and β that are used in the fitting, the fit with $\gamma_e=0$ clearly lags behind the data, especially at the first half cycle of vibration. The amount of lag is about 18°, the same as the value obtained in our earlier analysis using a damped harmonic oscillator model.[39] Our results contradict the claim in a recent publication[42] that electronic thermal stress in low excitation conditions is negligible, and cannot be measured and used for the accurate determination of electronic Grüneisen constant. Another interesting finding revealed in the simulation is that the triangle wave form of the average lattice expansion in real space (Fig. 4) is smeared out after converting into reciprocal space (Fig. 5). We attribute this to inhomogeneous expansion of the film. The difference of the displacement (vertical axis in Fig. 2) between two neighboring lattice positions (horizontal axis) gives the expansion at this specific lattice location. For a homogeneous expansion, the displacement is a linear function of lattice position. The deviation from this linear relation displayed in the dashed curves at 4, 5, and 6 ps delay times indicates an inhomogeneous lattice expansion across the film during this early stage.

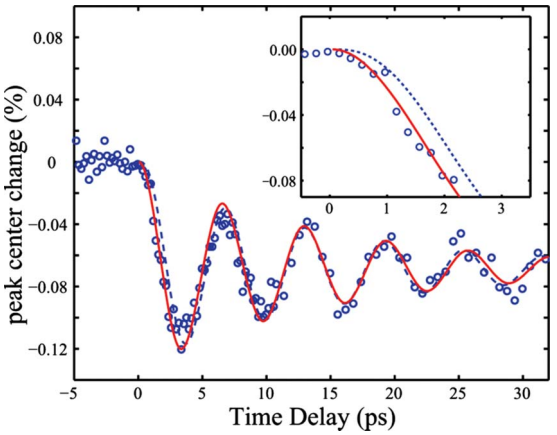

FIG. 5. (Color online) Comparison of the simulation results with experimental data. Circles are the FED experiment data points, solid line is the 1D model fit, and the dashed line is the 1D fit where electronic thermal stress is excluded. The inset is the magnified view near the time zero.

IV. CONCLUSIONS

In summary, we have deduced a one-dimensional model to simulate coherent lattice motion generated by ultrafast heating. Using this simulation, both the displacement and expansion at each lattice site along the 1D atomic chain can be traced as a function of delay time. Moreover, we show that the electronic thermal stress is responsible for driving the lattice motion at the early stage, with the extent depending on the values of the electronic Grüneisen constant,

electron-phonon thermalization time and the period of coherent vibration. Under favorable conditions, this electronic thermal stress results in a phase lead in coherent lattice vibration with respect to that induced only by lattice heating alone. These results agree very well with our FED experimental data obtained in the study of ultrafast heating of freestanding metal films.

ACKNOWLEDGMENTS

This work was supported by the National Science Foundation under Grant No. DMR-0606431. J.L. and X.W. would also like to thank National High Magnetic Field Laboratory for partial support.

*Author to whom correspondence should be addressed; jcao@magnet.fsu.edu

[1] C. Thomsen, H. T. Grahn, H. J. Maris, and J. Tauc, Phys. Rev. B **34**, 4129 (1986).
[2] O. B. Wright, Phys. Rev. B **49**, 9985 (1994).
[3] G. L. Eesley, B. M. Clemens, and C. A. Paddock, Appl. Phys. Lett. **50**, 717 (1987).
[4] G. V. Hartland, Annu. Rev. Phys. Chem. **57**, 403 (2006).
[5] N. Del Fatti, C. Voisin, D. Christofilos, F. Vallee, and C. Flytzanis, J. Phys. Chem. A **104**, 4321 (2000).
[6] W. Huang and M. A. El-Sayed, Eur. Phys. J. Spec. Top. **153**, 325 (2008).
[7] J. C. Wang and C. L. Guo, Phys. Rev. B **75**, 184304 (2007).
[8] N. Gedik, D. S. Yang, G. Logvenov, I. Bozovic, and A. H. Zewail, Science **316**, 425 (2007).
[9] C. Y. Ruan, V. A. Lobastov, F. Vigliotti, S. Y. Chen, and A. H. Zewail, Science **304**, 80 (2004).
[10] C. V. Shank, R. Yen, and C. Hirlimann, Phys. Rev. Lett. **50**, 454 (1983).
[11] H. W. K. Tom, G. D. Aumiller, and C. H. Britocruz, Phys. Rev. Lett. **60**, 1438 (1988).
[12] K. Sokolowski-Tinten, J. Bialkowski, and D. von der Linde, Phys. Rev. B **51**, 14186 (1995).
[13] H. Park, X. Wang, S. Nie, R. Clinite, and J. Cao, Phys. Rev. B **72**, 100301 (2005).
[14] C. Y. Ruan, D. S. Yang, and A. H. Zewail, J. Am. Chem. Soc. **126**, 12797 (2004).
[15] C. Rose-Petruck *et al.*, Nature (London) **398**, 310 (1999).
[16] A. M. Lindenberg *et al.*, Phys. Rev. Lett. **84**, 111 (2000).
[17] H. J. Lee *et al.*, Phys. Rev. B **77**, 132301 (2008).
[18] C. W. Siders *et al.*, Science **286**, 1340 (1999).
[19] B. J. Siwick, J. R. Dwyer, R. E. Jordan, and R. J. D. Miller, Science **302**, 1382 (2003).
[20] G. Sciaini *et al.*, Nature (London) **458**, 56 (2009).
[21] R. M. White, J. Appl. Phys. **34**, 3559 (1963).
[22] S. H. Nie, X. Wang, J. J. Li, R. Clinite, and J. M. Cao, Appl. Phys. Lett. **94**, 166101 (2009).
[23] K. Harumi, NDT Int. **19**, 315 (1986).
[24] H. Yim and Y. Sohn, IEEE Trans. Ultrason. Ferroelectr. Freq. Control **47**, 549 (2000).
[25] R. J. von Gutfeld and R. L. Melcher, Appl. Phys. Lett. **30**, 257 (1977).
[26] C. J. K. Richardson and J. B. Spicer, Appl. Phys. Lett. **80**, 2895 (2002).
[27] S. I. Anisimov, B. L. Kapeliovich, and T. L. Perel'man, Zh. Eksp. Teor. Fiz. **66**, 776 (1974).
[28] P. B. Allen, Phys. Rev. Lett. **59**, 1460 (1987).
[29] C. K. Sun, F. Vallee, L. H. Acioli, E. P. Ippen, and J. G. Fujimoto, Phys. Rev. B **50**, 15337 (1994).
[30] H. Park, X. Wang, S. Nie, R. Clinite, and J. Cao, Solid State Commun. **136**, 559 (2005).
[31] G. R. Stewart, Rev. Sci. Instrum. **54**, 1 (1983).
[32] E. D. Palik, *Handbook of Optical Constants of Solids* (Academic, Orlando, U.S.A., 1985).
[33] H. E. Elsayed-Ali and T. Juhasz, Phys. Rev. B **47**, 13599 (1993).
[34] R. J. Stoner and H. J. Maris, Phys. Rev. B **48**, 16373 (1993).
[35] R. J. Stevens, A. N. Smith, and P. M. Norris, J Heat Transfer **127**, 315 (2005).
[36] A. Cavalleri *et al.*, Phys. Rev. Lett. **85**, 586 (2000).
[37] D. G. Cahill, W. K. Ford, K. E. Goodson, G. D. Mahan, A. Majumdar, H. J. Maris, R. Merlin, and S. R. Phillpot, J. Appl. Phys. **93**, 793 (2003).
[38] E. T. Swartz and R. O. Pohl, Rev. Mod. Phys. **61**, 605 (1989).
[39] S. H. Nie, X. Wang, H. Park, R. Clinite, and J. M. Cao, Phys. Rev. Lett. **96**, 025901 (2006).
[40] M. Perner, S. Gresillon, J. Marz, G. von Plessen, J. Feldmann, J. Porstendorfer, K. J. Berg, and G. Berg, Phys. Rev. Lett. **85**, 792 (2000).
[41] C. Kittel, *Introduction to Solid State Physics*, 7th ed. (Wiley, New York, 1996).
[42] J. Tang, Appl. Phys. Lett. **92**, 011901 (2008).
[43] T. H. K. Barron, J. G. Collins, and G. K. White, Adv. Phys. **29**, 609 (1980).
[44] K. O. Mclean, C. A. Swenson, and C. R. Case, J. Low Temp. Phys. **7**, 77 (1972).